13 October 2017

Enhanced Grain-boundary Emission Lifetime and Additive Induced Crystal Orientation in One-Step Spin-Coated Mixed Cationic (FA/MA) Lead Perovskite Thin Films Stabilized by Zinc Iodide Doping

Loreta A. Muscarella,[1] Dina Petrova,[1] Rebecca Jorge Cervasio,[1] Aram Farawar,[1] Olivier Lugier,[1] Charlotte McLure,[1] Martin J. Slaman,[2] Junke Wang,[3] Elizabeth von Hauff,[2] René M. Williams[*1]

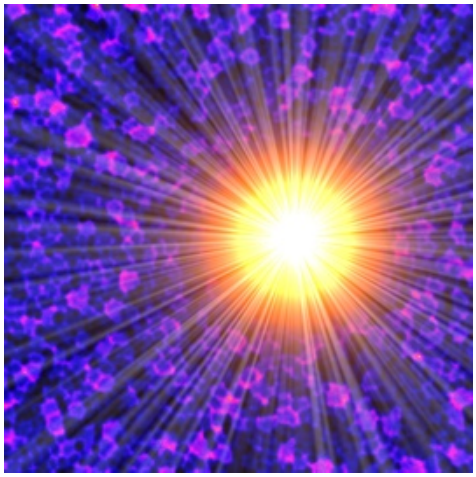

Table of Content picture.

[1]Molecular Photonics Group, Van't Hoff Institute for Molecular Sciences (HIMS), Universiteit van Amsterdam, Science Park 904, 1098 XH Amsterdam, Netherlands
[2] Department of Physics and Astronomy, Vrije Universiteit, de Boelelaan 1081, 1081 HV Amsterdam, Netherlands
[3]Molecular Materials and Nanosystems, Eindhoven University of Technology, P.O. Box 513, 5600 MB Eindhoven, Netherlands

Abstract:
Mixed cationic lead perovskites containing formamidinium and methylammonium can be stabilized by incorporating ZnI_2 as an "internal desiccant". Next to prolonged stability under ambient conditions we show with XRD that the use of an additive, 3-chloropropyl ammonium chloride, influences crystal formation by orienting the crystals. These ~500 nm crystals show individual photoluminescent behavior in thin films and have a longer photoluminescence lifetime at the grain boundaries as compared to the center of the crystal or relative to un-doped materials without the additive made under identical conditions. Charges recombine slower at the edges of the crystals as observed with confocal laser scanning microscopy. The material can also be prepared as a black precursor powder by a solid-solid reaction under ambient conditions.

Corresponding author: **r.m.williams@uva.nl**

Keywords: photovoltaics, semiconductors, hybrid inorganic solar cell materials, perovskite solar cells**,** crystal-grain boundary effects**,** confocal microscopy**,** formamidinium, methylammonium**,** 3-chloropropylammonium chloride

Introduction

The surging rise of the power conversion efficiency of perovskite solar cells (PSC) from 3.8%[1] to 22.1%[2] has shaken up the scientific photovoltaic community.[3, 4] Improved methods for perovskite thin film formation, new solar device architectures with optimal performance and shifting the band gap to the maximum and increasing efficiency towards[5] (or beyond) the Shockley-Queisser[6] (SQ) limit as well as improving stability are the current challenges in this field.[7] High band gap perovskites that make optimal tandem-cell combinations[8, 9] with state of the art commercial silicon solar cells could also propel the field even further. Comprehensive understanding and control of the inherent (photo)chemical properties and stability of these intriguing materials is paramount for progress.[10]

The chemical landscape of black perovskites for solar cells is surprisingly limited, with basically nine main components that can be applied: methylammonium (MA), formamidinium (FA), cesium(I), rubidium(I) (the monovalent cations), Pb(II) and Sn(II) as divalent species and chloride, bromide and iodide as the anions. However, several dopants and film forming additives can also be applied (*vide infra*). From the intrinsic properties of $MAPbI_3$ and $FAPbI_3$ it can be concluded that as pure materials, they do not have the right chemical stability and properties for industrial application in solar cells due to their phase-behavior.[11] The $FAPbI_3$ black phase. interconverts to the yellow phase in a couple of weeks at RT.[12]

Incorporation of a small amount of bromide (or chloride) influences the phase-changes while the band gap can remain unchanged, as already reported for $MAPbI_{2.66}Br_{0.34}$ by Weber in 1978[13] (who also reported on ambient stability of orange $MAPbBr_3$ and colorless $MAPbCl_3$). However, chloride components in the precursor solutions tend to be mainly eliminated as HCl vapour (or as CH_3NH_3Cl) during the annealing step through an intermediate phase, if an excess iodide is present (less than 1% chloride in final phase).[14] The monovalent cation in black lead perovskites can be methylammonium, formamidinium, cesium or rubidium. The most recent power conversion efficiency (PCE) records were obtained with (FA/MA) double (22.1% and 20.2%),[2, 15] (FA/MA/Cs) triple (21.1%)[16] and (FA/MA/Cs/Rb) quadruple (21.6%)[17] mixed mono-cationic lead iodide materials. Incorporation of ammonium ions such as guanidinium[18] or tetramethylammonium[19] leads to yellow non-perovskite type structures, in accordance with their Goldschmidt factors. Sofar Sn(II) is the only divalent metal ion that can result in similar black semiconductors with the same electron and hole conducting properties. Computational studies[20] also indicate that "the Pb^{2+} ion plays a paramount role in the optical properties of these systems", indicating that the properties of Pb(II) (and Sn(II)) are unique (perhaps as unique as their Group XIV companions carbon and silicon) and cannot easily be replaced in these perovskites.

Doping of silicon is quintessential for its application in solar cells, therefore it is tempting to dope Pb(II) perovskites thin films with various other ions. Cu(I), Na(I), and Ag(I)[21] as well as Au(III), In(III) and Bi(III),[22] and Sr(II)[23] have been applied as dopants. To our knowledge, Zn(II) has only recently been used as a dopant.[24, 25] It has been found that for these materials, doping levels around 2.5% give maximum effects on opto-electronic properties with minimal structural modification. Furthermore, the use of additives that influence film formation[26, 27] are of great importance.

By applying *Confocal Laser Scanning Microscopy* (CLSM)[28] the photoluminescence (PL) of microcrystalline perovskite films can be probed on a sub-micrometer scale with respect to emission intensity and lifetime. These CLSM studies have reported reduced PL lifetimes at the grain boundaries. Individual behavior of

dark or bright crystal grains as well as crystal grain-boundary effects can be monitored and have been combined with electron microscopy[29] as well as conductive atomic force microscopy. [30] Correlating structural effects to emissive properties of perovskites is important because the SQ limit[6] is based on the absence of non-radiative charge decay at open circuit conditions of solar cell devices. Ideally, all charge at open circuit (or injected under LED conditions) in a device should decay radiatively (and 100% of the charges should be collected at the electrodes at short circuit conditions).[31] Highly photo- or electro-luminescent crystal grains or boundaries therefore imply better photovoltaic activity.

In this work we report that air-stable mixed cationic MA/FA Zn(II)-doped perovskite crystals can be preferentially oriented in thin films by using the additive 3-chloropropylammonium chloride (CPACl).[27] (This additive was used before, but no orientation effects were observed for $MAPbI_3$). Optical, confocal and scanning electron microscopy shows smooth, dense, homogenous films. CPACl is not detectable (with SEM-EDX) in the films after annealing and does not shift the band gap substantially (but 3-bromopropylammonium *bromide* does). Furthermore, doping with ZnI_2 (2.5%) leads to improved intrinsic stability of the material at ambient conditions. Steady state spectroscopy shows a $FAPbI_3$ type emission. CLSM shows crystal-grain specific behavior and a longer emission lifetime at the grain-boundaries, in agreement with surface functionalization by CPACl. The material can also be prepared as a black precursor powder by a solid-solid reaction (with grinding) under ambient conditions.

Experimental

PbI_2 (99%)[32], ZnI_2, CPACl, BPABr were obtained from Sigma-Aldrich. MABr, FAI were obtained from TCI. Substrates were cleaned with Hellmanex, acetone and isopropanol using sonication, carefully dried and then UV-ozone treated. XRD was obtained with a Brucker D8 Discover with VÅNTEC-1 detector and Cu source. An Agilent/HP 8453 UV-Visible Spectrophotometer was used for absorbance measurements, a Spex FluoroMax-3 for emission and a Dektak 150 from Veeco for film thickness. An Olympus BX60 optical microscope was used. Confocal microscopy images were made with a Micro Time 200 (PicoQuant) with a SuperContinuum NKT Photonics laser operating at 9 MHz for excitation. A Field Emission SEM, Jeol JSM-6301F, equipped with a EDAX: Genesis Apex2 system (Apollo 10+) detector for elementary analysis was applied. Further experimental details on materials, instruments and procedures are provided in the Supporting Information (SI page S1 to S25).

Results and discussion

The main material discussed in this paper can be described using extended ABX_3 nomenclature $(A_{1-x}A'_x)(B_{1-y}B'_y)(X_{3-z}X'_z)$ - [Add] with the additive used in square brackets. $(FA_{0.85}MA_{0.15})(Pb_{0.975}Zn_{0.025})(I_{2.85}Br_{0.15})$-[CPACl] implying that the precursor solution used to make the material contains mainly formamidinium as the monovalent cation and 15% methylammonium. The main metal constituent is lead, but it is doped with 2.5% Zn(II). The main halide is iodide, but bromide is also present. The amount of 3-chloropropylammonium in the final material is currently unknown, as well as the amount of chloride.

Aging at ambient conditions of drop casted or spin coated MABr/FAI/PbI_2 films with randomly selected dopants (such as CuI, CuI_2, NiI_2, PdI_2, $tMAPbI_3$) led to rather unstable films (see S4). However, the application of ZnI_2 as a dopant for these mixed cationic perovskites led to clear increased stability in air, by visual observation. Therefore, we applied this dopant (ZnI_2) further in combination with additives. Tests with different additives (such as 1,3- dichloropropane, 1,4-dichlorobutane, 1,6-dichlorohexane, benzylammonium iodide) visually indicated very good film formation with 3-chloropropylammonium chloride (CPACl). CPACl also clearly improves solubility of PbI_2 in DMF, as also observed for other additives.[33] Experiments were directed at the effects of the CPACl-additive and ZnI_2 doping of MA/FA mixed cationic lead perovskites thin films.

Spincoating. Thin films on clean ITO with a very good visual, optical microscopy and Scanning Electron Microscopy appearance were made by one-step spincoating method. The presence of 3-chloropropylammonium chloride (CPACl, 0.4 M) in the fresh precursor solution (1.1 M PbI_2, (1.02 M FAI + 0.18 M MABr) in DMF induces an immediate darkening of the layer at the start of the spin-coating (which normally does not occur for $MAPbI_3$ or MA/FA-Pb-I_xBr_y). Ethylacetate was used as the anti-solvent, sprayed within ca. 0.1 s over the precursor layer after 15 s spinning at a fixed height of 3 cm under ambient conditions.[34] Annealing was performed for 5 minutes at 70 ˚C, followed by 15 minutes at 100 ˚C. Thickness was determined to be ~300 nm measured with a Dektak 150. This results in reproducible thin film formation under ambient conditions.[35] Films made in this way have a black appearance, dark brown when viewed in transmission against light. Thicker drop-casted films have a silvery "silicon-like" appearance (top) and black on the ITO site (bottom) see supporting information (S5). 0.4 M is the optimized CPACl concentration (see S6-S7).

Stability. In contrast to most black perovskite materials which degrade within minutes, days or weeks under ambient conditions into a yellow or white appearance,[36] our Zn(II) doped spin-coated films made with the 3-chloropropylammonium chloride (CPACl) additive remain black without substantial loss of sharp XRD features even after 60 days at ambient (Dutch) indoor conditions (see S8). Figure 1A/B shows typical examples observed for most perovskites (A) as compared to ($FA_{0.85}MA_{0.15}$) ($Pb_{0.975}$ $Zn_{0.025}$) ($I_{2.85}Br_{0.15}$)-[CPACl] shown in figure 1B. Our perovskite layers directly spin-coated on ITO remain more stable as compared to layers directly made on TiO_2. On PEDOT-PSS however, the material is also stable (see S9). The surface properties (acidities and energies) are of direct influence on perovskite layer stability,[37] as also observed by us for other perovskites layers made without the CPACl additive. Interestingly, ZnI_2 is a very hygroscopic material, but seems to show inverted behavior as a dopant in perovskites.

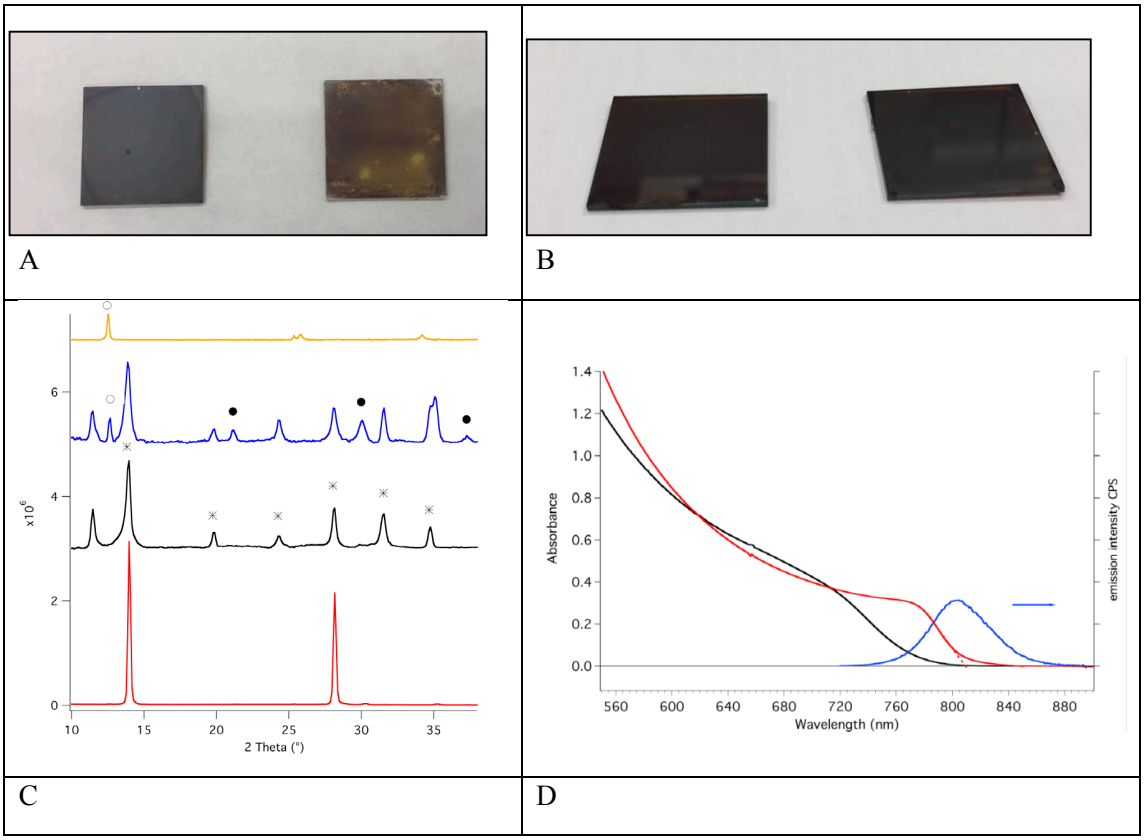

Figure . 1

*Visual effect of aging at ambient conditions of perovskite films. Newly prepared (left) and 30 days old (right) thin films of **A)** $(FA_{0.85}MA_{0.15})(Pb)(I_{2.85}Br_{0.15})$. Degradation starts in one week showing a progressive color change from black to light-yellow after 30 days. **B)** $(FA_{0.85}MA_{0.15})$ $(Pb_{0.975}$ $Zn_{0.025})$ $(I_{2.85}Br_{0.15})$ thin films made with CPACl additive remain the same black thin films after 30 days aging.*

***C**. XRD diffractograms of three perovskite thin films with varying constitution, together with PbI_2 (yellow):*
$(FA_{0.85}MA_{0.15})(Pb_{0.95}Zn_{0.05})(I_{2.85}Br_{0.15})$: *(5% ZnI_2, blue),*
$(FA_{0.85}MA_{0.15})(Pb_{0.975}Zn_{0.025})(I_{2.85}Br_{0.15})$: *(2.5% ZnI_2, black),*
$(FA_{0.85}MA_{0.15})(Pb_{0.975}Zn_{0.025})(I_{2.85}Br_{0.15})$-[CPACl]: *(2.5% ZnI_2 and additive, red).*
Intensity (y-axis) is in arbitrary units. Scaling is purely for visual clarity.

***D**. UV-Vis absorption spectra of layers made with BPABr (black) and with CPACl-additives (red). Emission spectrum of* $(FA_{0.85}MA_{0.15})(Pb_{0.975}Zn_{0.025})(I_{2.85}Br_{0.15})$-[CPACl] *(blue) shows typical MA/FA perovskite peak. The red dotted line indicates a band gap estimate (at 810 nm). The bromide is incorporated into the material, enlarging the band gap. The chloride is mainly eliminated during annealing.*

XRD. Figure 1C shows XRD of thin films on ITO of three different compositions and PbI_2. Whereas the strongest peak at 12.55˚of PbI_2 is present in the perovskite layer doped with 5% ZnI_2, its intensity is strongly reduced upon 2.5% doping, and typical peaks (at 11.47˚, 13.96˚, 19.87˚, 24.27˚, 28.16˚, 31.57˚, 34.77˚) are present. This would suggest the presence of mainly the alpha phase and some delta phase (11.47˚) of $FAPbI_3$[38] (mainly tetragonal structure).[11] The CPACl additive induces crystal orientation and a perfectly cubic structure as only the specific cubic perovskite diffractions at 13.96˚ and 28.16˚ remain. The determination of crystal orientation with XRD has been reported before,[15] but using a different, less generic method and for different perovskite compositions[39] and not with this additive. The absence of any diffraction relating to PbI_2 or ZnI_2 implies that the Zn(II) is incorporated into the lattice of the bulk material, taking the same place as the Pb(II). The homogeneous phase implies that it is a solid alloy-type solution.

For $FA_{0.85}MA_{0.15})(Pb)(I_{2.85}Br_{0.15})$ we observe a FWHM of 0.29° for the diffraction peaks. The latter value reduces to 0.21° for $(FA_{0.85}MA_{0.15})(Pb_{0.975}Zn_{0.025})(I_{2.85}Br_{0.15})$-[CPACl], indicating larger (and oriented) crystals, while the cell parameter = 6.343 Å. Using the additive as a bromide salt results in diffractions at 14.10° and 28.41° (cell parameter of 6.280 Å) and again slightly wider peaks. (0.26°). Clearly a lattice contraction is observed for the BPABr additive (see S10), because of bromide incorporation into the lattice, also indicated by the band gap shift (see UV-Vis section). Interestingly, we observe a similar orientation effect when the ITO is covered with PEDOT:PSS (see S9), implying potential device application.

Mixing the white and yellow solid components (PbI_2, FAI, MABr, ZnI_2 and CPACl) in a vial by shaking induces a solid-solid reaction turning the material partly brown/black. The reaction can be completed by grinding in a marble mortar under ambient conditions yielding a black shiny material (see S11). This indicates thermodynamics is in favor of a black perovskite phase for this composition, which we can consider a precursor powder.

UV-Vis absorption and emission The band gap of $(FA_{0.85}MA_{0.15})$ $(Pb_{0.975}$ $Zn_{0.025})$ $(I_{2.85}Br_{0.15})$-[CPACl] is set around 810 nm (see Fig. 1D), as expected for a FA/MA perovskite containing Pb(II) and mainly iodide. Clearly, the excess of chloride is not incorporated to a large extent. Relative to spin-coated layers of $(FA_{0.85}MA_{0.15})(Pb)$ $(I_{2.85}Br_{0.15})$ made and measured in the same conditions, the emission intensity is enhanced by a factor of ~23 by the Zn(II) incorporation and the action of the additive CPACl. In contrast, the use of a very similar bromide additive (BPABr = 3-bromopropylammonium bromide) results in a strong band gap shift (to a higher energy), indicating incorporation of the bromide in the lattice. This is also reflected in the XRD (see S10), resulting in a lattice contraction (from 6.343 Å (with 3-CPACl) to 6.280 Å (with 3-BPABr). However, crystal orientation is still observed (see S10).

Microscopy. Figure 2 shows optical and Scanning Electron microscopy images of layers of $(FA_{0.85}MA_{0.15})$ $(Pb_{0.975}$ $Zn_{0.025})$ $(I_{2.85}Br_{0.15})$ on ITO, made with CPACl. All methods indicate a smooth, dense, compact and homogeneous pinhole-free layer. Feature sizes are in the order of 500 nm in all images. With SEM it is possible to follow the film formation, showing an increase in film density during annealing. In this way an optimal annealing time and temperature can be obtained. Furthermore, high resolution images of our films show clear straight crystal facets (see figure 2C). This agrees with the high crystalline nature of the spin-coated films and the crystal orientation. It is likely that any contact between straight crystal facets of two crystal grains will influence grain boundary behavior. (see *confocal microscopy)*. EDX of these films clearly shows the presence of Zn, Br, Pb and I (see S12).

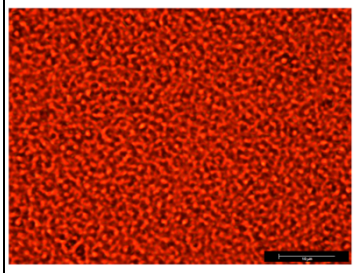	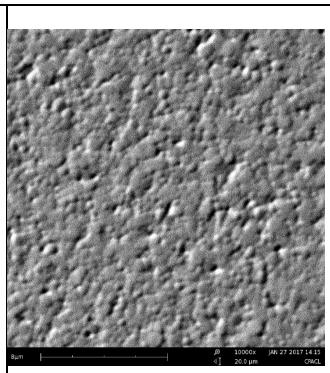	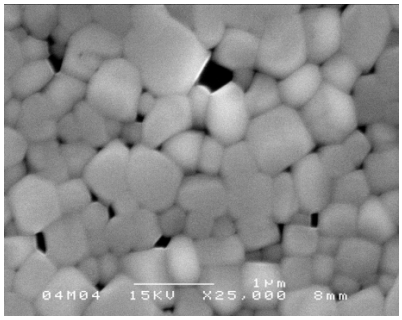
A	B	C

Figure 2.
Microscopy images of thin films of $(FA_{0.85}MA_{0.15})$ $(Pb_{0.975}\ Zn_{0.025})$ $(I_{2.85}Br_{0.15})$ *made with CPACl additive.* ***A)*** *Optical micrograph in transmission. Scale bar is 10 µm.* ***B)*** *SEM image. Scale bar is 8 µm. All images display a compact dense homogenous pinhole-free layer.* ***C)*** *High resolution SEM, showing clear straight touching crystal facets with square and pentagonal crystallites. Scale bar is 1 µm. Crystals are random in x-y plane, but show z-orientation.*

Confocal Microscopy The CLSM shows the presence of a uniform grain size of ca. 500 nm (with XRD indicating crystal orientation, *vide infra*). In general, the emission intensity is stronger in the center of the grains and weaker emission intensity is observed at the grain-boundaries (indicated by a darker rim color). In particular, the FLIM (Fluorescence Lifetime Imaging Microscopy) shows striking lighter-colored grain-boundaries, corresponding to crystal edges with a longer emission lifetime (but with lower emission intensity). Such grain boundary effects have been reported with high-resolution photoconductive AFM.[30] The CLSM shows clustering of low intensity grains, implying inter-grain charge coupling and/or surface coupling. Such effects are also discernable in the FLIM image. Zooming into a comparison of CLSM and FLIM clearly shows the correlation between long lifetime with low intensity and short lifetime with strong emission intensity (fig. 3C and 3D). ImageJ processed intensity divided by lifetime images present enhanced visualization of the difference in emissive properties of the grain-centers and grain-boundaries (fig. 3E) and the regular pattern of crystallites with square and pentagonal shapes.
In figure 3F two emission-decay traces (with bi-exponential fit) show the typical lifetime-difference between the crystal grain-centers and the crystal grain-boundaries, the latter showing the longer component (fit data: grain center: 1.2 ns (0.35), 3.2 ns (0.65); grain boundary: 1.3 ns (0.65), 8.5 ns (0.35)). Our observations show a slower charge recombination at the crystal-boundaries. This implies crystal-surface passivation by CPACl, thereby reducing the rate of charge recombination at surface states.

This is strikingly different from observations made on $MAPbI_3$ films, where a low intensity and a shorter PL lifetimes at the grain-boundaries were reported.[29] CLSM without the CPACl additive (see S13-S14) is in agreement with these observations. Clearly, the additive has a strong influence on the PL. Furthermore, it has been reported that exposure of perovskite films to pyridine or thiophene can result in emission enhancement by interaction with vacancies.[29, 40] We attribute the extended PL lifetime to similar effects exerted by the CPACl additive incorporated in the film during its manufacture.

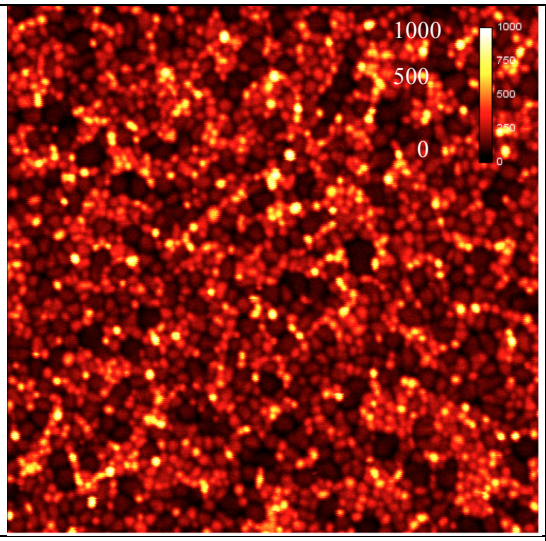
1000
500
0
1000
750
500
250
0

A

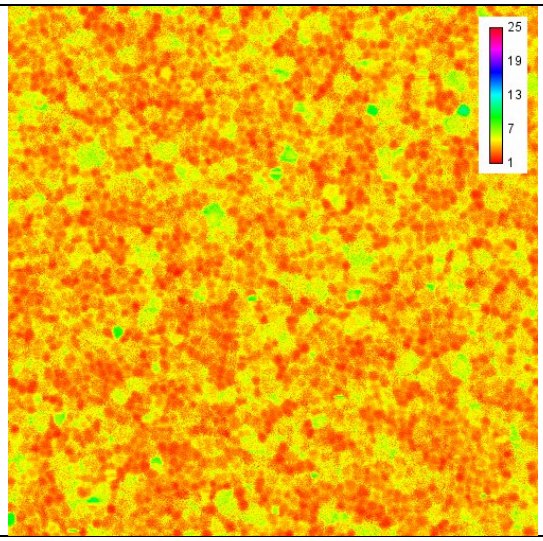
25
19
13
7
1

B

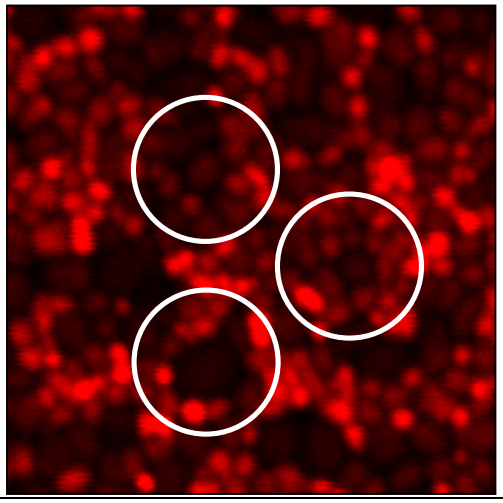

C

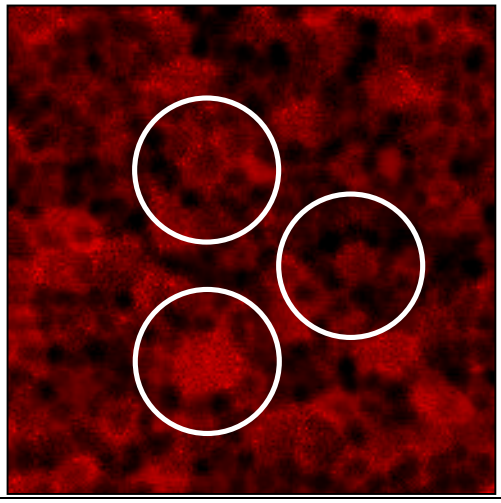

D

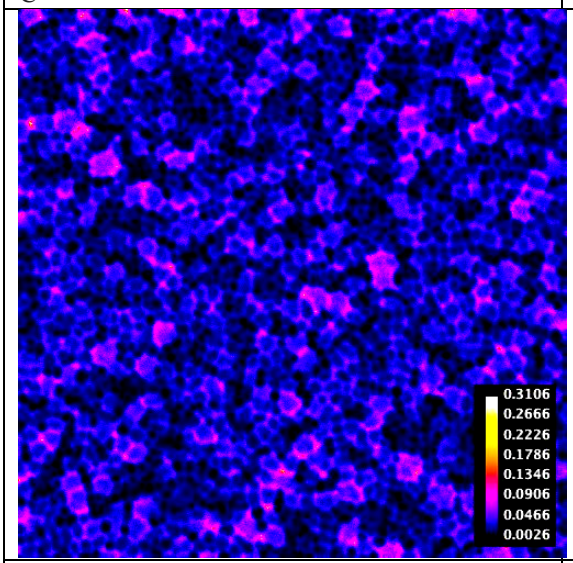
0.3106
0.2666
0.2226
0.1786
0.1346
0.0906
0.0466
0.0026

E

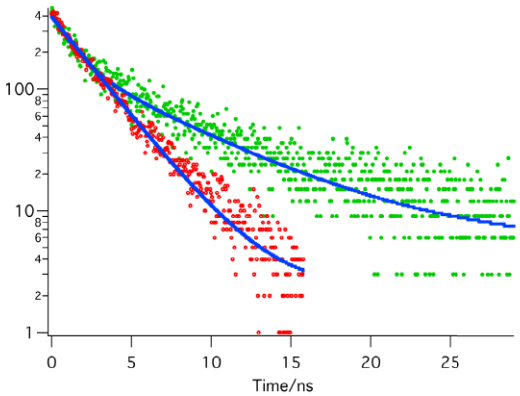
100
10
1
0
5
10
15
20
25
Time/ns

F

Figure 3

***A**: Confocal fluorescence image showing emission intensity distribution of* $(FA_{0.85}MA_{0.15})(Pb_{0.975}Zn_{0.025})(I_{2.85}Br_{0.15})$-[CPACl]. *Inset shows relative intensity scale.* Image dimensions: *20 × 20 µm.* ***B**: Confocal fluorescence image (FLIM) showing fluorescence lifetime distribution (average arrival time). Inset shows relative lifetime-color-scale in ns. Note the light yellow rims on the crystal faces indicating a longer emission lifetime at the crystal boundary, indicating passivation. Image dimension: 20 × 20 µm.* ***C+D**: Accentuation of the correspondence of "low intensity emission"-"long emissive lifetime" regions within the film. Intensity (**A**) vs. Lifetime (**B**) images. Image is 7.6 × 7.6 µm (1 pixel is 40 nm). (Data taken from Figure **3A/B**).* ***E**: Confocal microscopy image obtained by dividing the lifetime-image by the intensity-image (see also fig. **3A/B**), thereby accentuating the grain boundary area's, as processed with Image-J (lifetime/INT, fire-color coding). The network of light blue lines highlights the omnipresent grain boundary effect. Pink spots are characterized by a very low emission intensity and long emissive lifetime. Image dimension is 20 × 20 µm.*

***F**: Emission decay curves of crystal-grain centers (red data) and grain-bounderies (green data) together with bi-exponential fits (in blue)*

Summary
Our results indicate that FA/MA based lead perovskite materials for solar cells can be stabilized by ZnI_2 doping and crystal-oriented by the CPACl additive. The straightforward one step deposition makes this a more generally applicable method (as compared to, for example, the two-step method with PbI_2(DMSO).[15]

We propose that a gradual change of the ratio of (FA/MA) relative to CPACl (during spin-coating and annealing) induces a cooperative transition from a 2D to a 3D perovskite, inducing organization. A controlled ratio-change of similar components was reported[41] by Mitzi and co-workers (with Sn(II) and n-butylammonium). Figure 4 details their mechanism that can also be applied here.

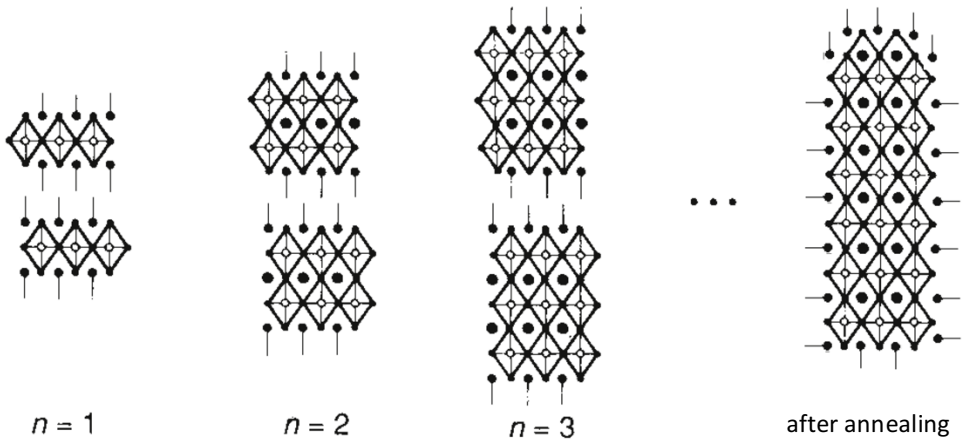

Figure 4.
Decreasing ratio of additive/perovskite during spin-coating and annealing leads to stacking of preformed crystalline units giving an organized and protected final product.). •— = *additive*, • = FA or MA, ◦ = *Pb(II), corners are halogenides*. *(Adapted from reference 43).*

Clearly, the alkyl tail as well as the amino group are essential components for the functioning of the additive. Systematic modulation of the chain length, halide anion and halide-substituent (or even the amino group) could improve the action of the additive, also for other perovskite precursor solutions.

Confocal microscopy with emission intensity and lifetime probing can give detailed information on sub~100 nm dimensions giving crystal-grain specific information on crystal-bulk and grain-boundary passivation and crystal grain-boundary matching. The enhanced lifetime observed here at the grain-boundaries implies slower charge recombination due to surface functionalization at the interfaces of $(FA_{0.85}MA_{0.15})(Pb_{0.975}\ Zn_{0.025})(I_{2.85}Br_{0.15})$ crystallites.

The sensitivity of black semiconducting perovskites implies that our approach of stabilization with ZnI_2 and orienting with CPACl may not be generic, but it is anticipated that stabilizing dopants and orienting additives can be found also for other perovskite precursor compositions.

Our material composition based on $(FA_{0.85}MA_{0.15})(Pb_{0.975}\ Zn_{0.025})(I_{2.85}Br_{0.15})$-[CPACl] can lead to further application of black perovskites for solar cells[42] with improved stability and processing at ambient conditions (a first un-optimized attempt yielding ~9% PCE, see S15-S17).

Supporting Information
Further information and experimental details are available with this manuscript.

Acknowledgements
We thank the Erasmus+ exchange program for supporting LAM, RJC, OL and CM. We thank Prof. Dr. Ir. R. A. J. Janssen for solar cell research facilities. We thank the Universiteit van Amsterdam for structural support.

References

[1] Kojima, A.; Teshima, K.; Shirai, Y.; Miyasaka, T.; "Organometal halide perovskites as visible-light sensitizers for photovoltaic cells". J. Am. Chem. Soc. 131, 6050–6051 (2009). DOI: 10.1021/ja809598r

[2] Yang, W. S.; Park, B.-W.; Jung, E. H.; Jeon, N. J.; Kim, Y. C.; Lee, D. U.; Shin, S. S.; Seo, J.; Kim, E. K.; Noh, J. H. et al. "Iodide management in formamidinium-lead-halide–based perovskite layers for efficient solar cells". Science 2017, 356, 1376–1379 DOI: 10.1126/science.aan2301

[3] See for example: Accounts of Chemical Research special issue "Lead Halide Perovskites for Solar Energy Conversion".
http://pubs.acs.org/page/achre4/solar_energy.html

[4] Hybrid perovskite's recent re-discovery indicates that the scientific community "missed" the highly promising solar application of these materials in the mid 1980's when these materials were first studied. Clearly, it also confronts us with the fact that we could still discover other brand new optimal solar cell materials.

[5] Eperon, G. E.; Leijtens, T.; Bush, K. A.; Prasanna, R.; Green, T.; Wang, J. T.-W.; McMeekin, D. P.; Volonakis, G.; Milot, R. L.; May, R.; Palmstrom, A.; Slotcavage, D. J.; Belisle, R. A.; Patel, J. B.; Parrott, E. S.; Sutton, R. J.; Ma, W.; Moghadam, F.; Conings, B.; Babayigit, A.; Boyen, H.-G.; Bent, S.; Giustino, F.; Herz, L. M.; Johnston, M. B.; McGehee, M. D.; Snaith, H. J. "Perovskite-Perovskite Tandem Photovoltaics with Optimized Bandgaps", Science 2016, 354, 861.
DOI:10.1126/science.aaf9717.

[6] Shockley, W.; Queisser, H.J.; "*Detailed Balance Limit of Efficiency of p-n Junction Solar Cells*", J. Appl. Phys., **1961**, 32, 510.

[7] Polman, A.; Knight, M.; Garnett, E.C.; Ehrler, B.; Sinke, W.C.; "Photovoltaic materials: Present efficiencies and future challenges", Science, 2016, 352, 6283

[8] Ergen, O.; Gilbert, S. M.; Pham, T.; Turner, S. J.; Tan, M. T. Z; Worsley, M. A.; Zettl, A. "Graded bandgap perovskite solar cells" Nat. Mater. 2016, 16, 522, DOI: 10.1038/nmat4795

[9] Bush, K. A.; Palmstrom, A. F.; Yu, Z. J.; Boccard, M.; Cheacharoen, R.; Mailoa, J. P.; McMeekin, D. P.; Hoye, R. L. Z.; Bailie, C. D.; Leijtens, T. et al. "23.6%-efficient Monolithic Perovskite/Silicon Tandem Solar Cells with Improved Stability" Nat. Energy 2017, 2, 17009 DOI: 10.1038/nenergy.2017.9

[10] a) Stoumpos, C. C.; Malliakas, C. D.; Kanatzidis, M. G. "Semiconducting Tin and Lead Iodide Perovskites with Organic Cations: Phase Transitions, High Mobilities, and Near-Infrared Photoluminescent Properties" Inorg. Chem. 2013, 52, 9019– 9038, DOI: 10.1021/ic401215x

b) Song, T.-B.; Yokoyama, T.; Stoumpos, C. C.; Logsdon, J.; Cao, D. H.; Wasielewski, M. R.; Aramaki, S.; Kanatzidis, M. G. "Importance of Reducing Vapor Atmosphere in the Fabrication of Tin-Based Perovskite Solar Cells" J. Am. Chem. Soc. 2017, 139, 836– 842, DOI: 10.1021/jacs.6b10734

c) Stoumpos, C. C.; Kanatzidis, M. G. "The Renaissance of Halide Perovskites and Their Evolution as Emerging Semiconductors" Acc. Chem. Res. 2015, 48, 2791–2802, DOI: 10.1021/acs.accounts.5b00229

[11] Baikie, T.; Fang, Y. N.; Kadro, J. M.; Schreyer, M.; Wei, F. X.; Mhaisalkar, S. G.; Graetzel, M.; White, T. J. "Synthesis and Crystal Chemistry of the Hybrid Perovskite $(CH_3NH_3)PbI_3$ for Solid-State Sensitised Solar Cell Applications" J. Mater. Chem. A 2013, 1, 5628– 5641, DOI: 10.1039/c3ta10518k.

[12] Gélvez-Rueda, M. C.; Renaud, N.; Grozema, F. C.; "Temperature Dependent Charge Carrier Dynamics in Formamidinium Lead Iodide Perovskite" J. Phys. Chem. C, Article ASAP 2017, DOI: 10.1021/acs.jpcc.7b09303

[13] Weber, D.; "$CH_3NH_3PbX_3$, a Pb(II)-System with Cubic Perovskite Structure", *Z. Naturforsch.*, 1978, 33b, 1443 - 1445.

[14] Yu, H.; Wang, F.; Xie, F.; Li, W.; Chen, J.; Zhao, N. "The role of chlorine in the formation process of ″CH3NH3PbI$_{3-x}$Cl$_x$ perovskite" Adv. Funct. Mater. 2014, 24, 7102– 7108 DOI: 10.1002/adfm.201401872.

[15] Yang, W.-S; Noh, J. H.; Jeon, N. J.; Kim, Y. C.; Ryu, S.; Seo, J.; Seok, S. I. "High-performance photovoltaic perovskite layers fabricated through intramolecular exchange" Science 2015, 348, 1234, DOI: 10.1126/science.aaa9272.

[16] Saliba, M.; Matsui, T.; Seo, J. Y.; Domanski, K.; Correa-Baena, J. P.; Nazeeruddin, M. K.; Zakeeruddin, S. M.; Tress, W.; Abate, A.; Hagfeldt, A.; Grätzel, M. "Cesium-Containing Triple Cation Perovskite Solar Cells: Improved Stability, Reproducibility and High Efficiency", Energy Environ. Sci. 2016, 9, 1989– 1997, DOI: 10.1039/C5EE03874J.

[17] Saliba, M.; Matsui, T.; Domanski, K.; Seo, J. Y.; Ummadisingu, A.; Zakeeruddin, S. M.; Correa-Baena, J. P.; Tress, W. R.; Abate, A.; Hagfeldt, A.; Graetzel, M.; "Incorporation of Rubidium Cations into Perovskite Solar Cells Improves Photovoltaic Performance", Science 2016, 354, 206–209, DOI: 10.1126/science.aah5557.

[18] Marco, N. D.; Zhou, H.; Chen, Q.; Sun, P.; Liu, Z.; Meng, L.; Yao, E.-P.; Liu, Y.; Schiffer, A.; Yang, Y. "Guanidinium: a Route to Enhanced Carrier Lifetime and Open-Circuit Voltage in Hybrid Perovskite Solar Cells". Nano Lett. 2016, 16, 1009– 1016, DOI: 10.1021/acs.nanolett.5b04060

[19] Liu, G.; Liu, J.; Sun, Z.; Zhang, Z.; Chang, L.; Wang, J.; Tao, X.; Zhang, Q. "Thermally Induced Reversible Double Phase Transitions in an Organic-Inorganic Hybrid Iodoplumbate $C_4H_{12}NPbI_3$ with Symmetry Breaking". Inorg. Chem. 2016, 55, 8025– 8030, DOI: 10.1021/acs.inorgchem.6b01143

[20] Filippetti, A.; Mattoni, A. "Hybrid perovskites for photovoltaics: Insights from first principles", Phys. Rev. B: Condens. Matter Mater. Phys. 2014, 89, 125203, DOI: 10.1103/PhysRevB.89.125203

[21] Abdi-Jalebi, M.; Dar, M. I.; Sadhanala, A.; Senanayak, S. P.; Franckevičius, M.; Arora, N.; Hu, Y.; Nazeeruddin, M. K.; Zakeeruddin, S. M.; Grätzel, M. et al. "Impact of Monovalent Cation Halide Additives on the Structural and Optoelectronic

Properties of $CH_3NH_3PbI_3$ Perovskite". Adv. Energy Mater. 2016, 6, 1502472 DOI: 10.1002/aenm.201502472.

[22] Abdelhady, A. L.; Saidaminov, M. I.; Murali, B.; Adinolfi, V.; Voznyy, O.; Katsiev, K.; Alarousu, E.; Comin, R.; Dursun, I.; Sinatra, L. et al. "Heterovalent Dopant Incorporation for Bandgap and Type Engineering of Perovskite Crystals". J. Phys. Chem. Lett. 2016, 7, 295– 301 DOI: 10.1021/acs.jpclett.5b02681.

[23] Pérez-del-Rey, D.; Forgács, D.; Hutter, E. M.; Savenije, T. J.; Nordlund, D.; Schulz, P.; Berry, J. J.; Sessolo, M.; Bolink, H. J. 'Strontium Insertion in Methylammonium Lead Iodide: Long Charge Carrier Lifetime and High Fill-Factor Solar Cells' , Adv. Mater. 2016, 28, 9839, DOI: 10.1002/adma.201603016

[24] Klug, M. T.; Osherov, A.; Haghighirad, A. A.; Stranks, S. D.; Brown, P. R.; Bai, S.; Wang, J. T. W.; Dang, X.; Bulović, V.; Snaith, H. J. "Tailoring Metal Halide Perovskites through Metal Substitution: Influence on Photovoltaic and Material Properties" Energy Environ. Sci. 2017, 10, 236– 246, DOI: 10.1039/C6EE03201J

[25] van der Stam, W.; Geuchies, J. J.; Altantzis, T.; van den Bos, K. H. W.; Meeldijk, J. D.; Aert, S. V.; Bals, S.; Vanmaekelbergh, D.; de Mello Donegá, C. "
Highly Emissive Divalent-Ion-Doped Colloidal $CsPb_{1-x}M_xBr_3$ Perovskite Nanocrystals through Cation Exchange" J. Am. Chem. Soc. 2017, 139, 4087– 4097, DOI: 10.1021/jacs.6b13079

[26] Li, X.; Ibrahim Dar, M.; Yi, C.; Luo, J.; Tschumi, M.; Zakeeruddin, S. M.; Nazeeruddin, M. K.; Han, H.; Gratzel, M. "Improved Performance and Stability of Perovskite Solar Cells by Crystal Crosslinking with Alkylphosphonic Acid Omega-ammonium Chlorides" Nat. Chem. 2015, 7, 703– 711, DOI: 10.1038/nchem.2324

[27] Wang, Y.; Song, N.; Feng, L.; Deng, X. Effects of Organic Cation Additives on the Fast Growth of Perovskite Thin Films for Efficient Planar Heterojunction Solar Cells"". ACS Appl. Mater. Interfaces 2016, 8, 24703–24711, DOI: 10.1021/acsami.6b06633.

[28] Siekierzycka, J. R.; Hippius, C.; Wurthner, F.; Williams, R. M.; Brouwer, A. M. "Polymer Glass Transitions Switch Electron Transfer in Individual Molecules". J. Am. Chem. Soc. 2010, 132, 1240– 1242

[29] deQuilettes, D. W.; Vorpahl, S. M.; Stranks, S. D.; Nagaoka, H.; Eperon, G. E.; Ziffer, M. E.; Snaith, H. J.; Ginger, D. S. "Impact of Microstructure on Local Carrier Lifetime in Perovskite Solar Cells", Science 2015, 348, 683– 686, DOI: 10.1126/science.aaa5333

[30] Eperon, G. E.; Moerman, D.; Ginger, D. S. "Anticorrelation between Local Photoluminescence and Photocurrent Suggests Variability in Contact to Active Layer in Perovskite Solar Cells" ACS Nano 2016, 10, 10258– 10266, DOI: 10.1021/acsnano.6b05825

[31]Stranks, S. D. "Nonradiative Losses in Metal Halide Perovskites". ACS Energy Lett., 2017, 2 (7), 1515–1525. DOI: 10.1021/acsenergylett.7b00239

[32] NOTE: Our experience is that 99.999% PbI_2 from Sigma Aldrich gives solubility problems and cannot be used.

[33] Lee, H. S.; Kim, A.; Kwon, H. C.; Yang, W. S.; Oh, Y. J.; Lee, D. H.; Moon, J. "Retarding Crystallization during Facile Single Coating of NaCl-Incorporated Precursor Solution for Efficient Large-Area Uniform Perovskite Solar Cells". ACS Appl. Mater. Interfaces 2016, 8, 29419– 29426 DOI: 10.1021/acsami.6b08783.

[34] Vaporization of components in the precursor solution is very different in a glove-box (and influenced by its settings) as compared to ambient conditions and therefore will give different results.

[35] Without automated spin-coaters, with which all parameters can be optimized and fully specified for every perovskite precursor composition, making good layers remains a bit of a "craftsmanship".

[36] Wilderspin, T. J.; De Rossi, F.; Watson,T. M., "A simple method to evaluate the effectiveness of encapsulation materials for perovskite solar cells", Sol. Energy, 2016, 139, 426–432. DOI:10.1016/j.solener.2016.09.038

[37] Yang, J. L.; Siempelkamp, B. D.; Mosconi, E.; De Angelis, F.; Kelly, T. L. "Origin of the Thermal Instability in $CH_3NH_3PbI_3$ Thin Films Deposited on ZnO", Chem. Mater. 2015, 27, 4229– 4236, DOI: 10.1021/acs.chemmater.5b01598

[38] Jeon, N. J.; Noh, J. H.; Yang, W. S.; Kim, Y. C.; Ryu, S.; Seo, J.; Seok, S. I. "Compositional Engineering of Perovskite Materials for High-Performance Solar Cells", Nature 2015, 517, 476– 480, DOI: 10.1038/nature14133

[39] Oesinghaus, L.; Schlipf, J.; Giesbrecht, N.; Song, L.; Hu, Y.; Bein, T.; Docampo, P.; Müller-Buschbaum, P. "Toward Tailored Film Morphologies: The Origin of Crystal Orientation in Hybrid Perovskite Thin Films" Adv. Mater. Interfaces 2016, 3, 1600403 DOI: 10.1002/admi.201600403

[40] Noel, N. K.; Abate, A.; Stranks, S. D.; Parrott, E. S.; Burlakov, V. M.; Goriely, A.; Snaith, H. J. "Enhanced Photoluminescence and Solar Cell Performance Via Lewis Base Passivation of Organic-Inorganic Lead Halide Perovskites". ACS Nano 2014, 8, 9815– 21, DOI: 10.1021/nn5036476

[41] Mitzi, D. B.; Feild, C.; Harrison, W.; Guloy, A. "Conducting tin halides with a layered organic-based perovskite structure" Nature 1994, 369, 467– 469, DOI: 10.1038/369467a0

[42] A first attempt to incorporate this material into devices gave a PCE of 8.9% for a 300 nm thick layer. Optimization is clearly possible. Doubling concentrations doubles the layer thickness.